

## MODELING AND MODAL TESTING OF ANNULAR PLATES

Jorge A. B. Gripp\*<sup>1</sup>, Luiz C. S. Góes<sup>1</sup>, Airton Nabarrete<sup>1</sup>

<sup>1</sup>Instituto Tecnológico de Aeronáutica, São José dos Campos, Brazil  
jorge.gripp@gmail.com, goes@ita.br, nabarret@ita.br

**Keywords:** Annular plate, Kirchhoff plate, Modal analysis, Modal testing, Flexible bodies.

**Abstract.** *The purpose of this work is to model analytically the deformation of an elastic disc using a non-traditional radial discretization and compare the natural modes with other traditional mathematical models and with experimental modal model. Modeling of annular plates has a Closed-form solution (CFS), where radial modes are represented as Bessel functions and angular modes as sinusoidal functions. In order to reduce the computation time spent in this specific task, we used a different mathematical approach, replacing Bessel functions by B-Splines, which are polynomial functions. A finite dimensional model of the plate deformation is derived using assumed modes method, separating the plate deflection in time and space. Explicit equations of motion are derived using Lagrangian approach. A modal testing of a typical annular plate was performed in order to obtain the modal parameters. Validation is done by comparing eigenfrequencies and eigenmodes from the proposed analytical method with those calculated using the Finite Element Method (FEM), using the CFS and with modal model of a real annular plate.*

## 1 INTRODUCTION

Plates are defined as plane structural elements with a small thickness compared to the planar dimensions. The aim of plate theory is to calculate the deformation and stresses in a plate subjected to loads. Common examples of plates are windows, walls and metallic discs [1]. As structural elements, plates are extensively used in the construction of aircraft, ships, automobiles and other vehicles [2].

Knowledge of the vibrations of structures was mostly limited to empirical descriptions of pendulums and stringed instruments until the development of calculus by Sir Isaac Newton and Gottfried Wilhelm Leibnitz in the late 1600's. The first instance in which the normal modes of continuous systems were determined involved the modes of a hanging chain, which were described in terms of Bessel functions by Daniel Bernoulli in 1732 [1]. Circa 1750 Leonhard Euler and Daniel Bernoulli were the first to put together a useful theory to describe the load-carrying and deflection characteristics of beams, known as Euler-Bernoulli beam theory. [3]

The beauty and intricacy of modal patterns were actually visualized in 1787 when Ernst Chladni developed the method of placing sand on a vibrating plate. The theory of vibrating plates was completed in 1850 by Gustav Kirchhoff [4], who closed the mathematical formulation through the variational treatment of boundary conditions. This first model of thin plate bending is known as the Kirchhoff plate or Kirchhoff-Love plate theory [5]. The theory takes advantage of the disparity in length scale to reduce the full three-dimensional continuum mechanics problem to a two-dimensional problem. Love [6] and Lamb [7] together with Rayleigh [8] form the basis of modern vibrating analysis.

Euler-Bernoulli beam theory and Kirchhoff-Love plate theory are the classical theories to represent deflection in a one-dimensional and two-dimensional form. More sophisticated theories were developed in order to take into account the shear deformation: Timoshenko beam theory [9] and Mindlin-Reissner plate theory [10-11].

The widespread of electronic computers in the early 1960's has made it feasible to simulate systems directly using finite element models (FEM). Although most vibration analysis of plates is done using finite element method (FEM) nowadays, some kinds of plates with high degree of symmetry can yet be calculated using analytical approaches, which consumes less computational effort. Modes of vibration of rectangular plates can be expressed in closed-form solution (CFS) as the multiplication of two trigonometric functions, each one depending on a coordinate in the plane of the plate. Circular and annular plates have more complex closed-form solutions, expressed in trigonometric functions in angular coordinate and Bessel functions in radial coordinate [2].

## 2 PLATE MODELING USING B-SPLINES

In this work we use an analytical approach to model the deformation of an annular plate subjected to flexural bending. The plate is represented using the Kirchhoff plate model, but B-spline functions are used to discretize the radial modes instead of Bessel functions. The Kirchhoff plate model is applicable to elastic plates that satisfy the following conditions:

- The plate is thin in the sense that the thickness  $h$  is small compared to the length  $2a$ , but not so thin that the lateral deflection becomes comparable to  $h$ , i.e.,  $0.2 < h/2a < 0.01$ .
- The plate thickness is either uniform or varies slowly so that three-dimensional stress effects are ignored.
- The plate is symmetric in fabrication about the mid-surface.
- The loads act perpendicular to the plate and are distributed over the plate surface areas of dimension  $h$  or greater.

- The support conditions are such that no significant extension of the mid-surface develops.

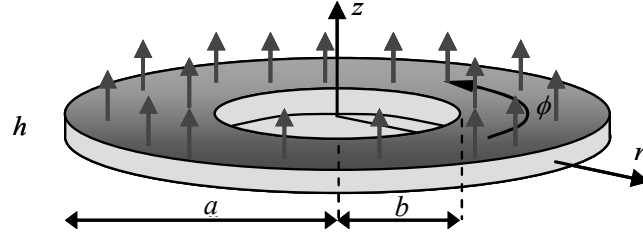


Figure 1: An annular plate subjected to flexural bending.

We use cylindrical coordinates to represent transverse deformation  $z(r, \varphi, t)$  of the elements of the plate as a function of the radius  $r \in [b, a]$ , the angle  $\varphi \in [0, 2\pi]$  and time  $t$ . Trigonometric functions ( $\bar{\Phi}(\varphi)$ ) in angular coordinate and B-Spline functions ( $\bar{R}(r)$ ) in radial coordinate are used to discretize the deformation. The bigger is the number of functions used, the more accurate will be the approximation.

The displacement  $z(r, \varphi, t)$  can be decomposed into space and time vectors, one referring to the geometry  $\bar{w}^T(r, \varphi)$  and the other to time  $\bar{q}^T(t) = [q_1 \ q_2 \ q_3 \ \dots]$ . The elements of the vector  $\bar{w}^T(r, \varphi) = [w_1 \ w_2 \ w_3 \ \dots]$  are all the combinations of multiplications between the elements of  $\bar{R}$  and  $\bar{\Phi} = [1 \ \sin \varphi \ \cos \varphi \ \sin 2\varphi \ \cos 2\varphi \ \sin 3\varphi \ \cos 3\varphi \ \dots]$ .

Inner ( $r=b$ ) and outer boundary conditions ( $r=a$ ) are implicitly defined when  $\bar{R}(r)$  functions are chosen. Each one can be Free (no restriction), Supported ( $\bar{R}(r=b)=0$ ) or Clamped ( $\bar{R}(r=b)=0$  and  $\frac{\partial \bar{R}}{\partial r}(r=b)=0$ ). Figure 2 shows  $R_1$ ,  $R_6$ , and  $R_7$  are discarded because they do not match Supported-Clamped boundary condition.

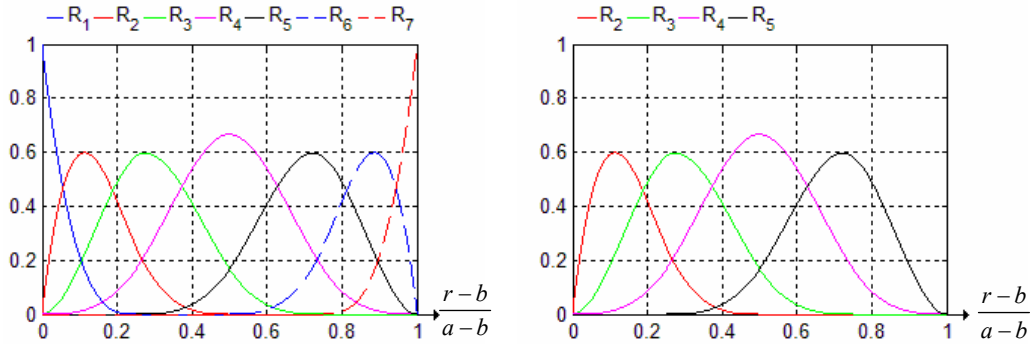


Figure 2: Cubic B-splines ( $k=3$ ). Left: plate Free-Free. Right: plate Supported-Clamped.

In order to derive the dynamic equations of a the annular plate, we can use the Euler-Lagrange equation (1), where  $T$  represents the kinetic energy and  $V$  the potential energy of the system [12-13].

$$\frac{d}{dt} \left( \frac{\partial T}{\partial \dot{q}} \right) + \frac{\partial V}{\partial q} - \frac{\partial T}{\partial q} = 0 \quad (1)$$

$$T = \frac{1}{2} \rho \cdot h \cdot \int_0^{2\pi} \int_b^a \left( \frac{\partial z}{\partial t} \right)^2 r \cdot dr d\varphi \quad (2)$$

$$V = \frac{D}{2} \int_0^{2\pi} \int_b^a \left\{ (z_{,rr} + \frac{1}{r^2} z_{,\varphi\varphi} + \frac{1}{r} z_{,r})^2 + 2(1-\nu) \left[ \left( \frac{1}{r} z_{,r\varphi} - \frac{1}{r^2} z_{,\varphi} \right)^2 - z_{,rr} \cdot \left( \frac{1}{r^2} z_{,\varphi\varphi} + \frac{1}{r} z_{,r} \right) \right] \right\} r \cdot dr \cdot d\varphi \quad (3)$$

Where  $D = \frac{E \cdot h^3}{12 \cdot (1-\nu^2)}$  is the bending rigidity of plate,  $\rho$  is the mass density,  $E$  is the

Young's modulus,  $\nu$  is the Poisson ratio,  $b$  is inner radius,  $a$  is outer radius,  $z_{,r\varphi} = \frac{\partial^2 z}{\partial r \partial \varphi}$ ,

$$\dot{\bar{q}} = \frac{\partial \bar{q}}{\partial t}, \text{ and } \ddot{\bar{q}} = \frac{\partial^2 \bar{q}}{\partial t^2}.$$

Solving the integrals of Lagrange Equation using Eq. (1) - (3) results on Eq. (4), where  $\mathbf{M}$  is the mass matrix and  $\mathbf{K}$  is the stiffness matrix of the system.

$$\mathbf{M} \cdot \ddot{\bar{q}} + \mathbf{K} \cdot \bar{q} = \bar{0} \quad (4)$$

Matrix  $\mathbf{M}$  depends on the first term of Lagrange equation (1) (derivative of the kinetic energy  $T$  with respect to  $\dot{\bar{q}}$ ),  $\mathbf{K}$  depends on the second term (derivative of the potential energy  $V$  with respect to  $\bar{q}$ ), and the third term is zero. Evaluating each element of  $\mathbf{M}$  and  $\mathbf{K}$ :

$$M_{ij} = \rho \cdot h \cdot \int_b^a R_c \cdot R_e \cdot r \cdot dr \int_0^{2\pi} \Phi_d \cdot \Phi_f \cdot d\varphi = \rho \cdot h \cdot I_{mr} \cdot I_{mphi} \quad (5)$$

$$K_{ij} = D \sum_{l=1}^{17} \left\{ \int_b^a c(l) \cdot \frac{r}{r^f} \cdot \frac{\partial^{\alpha(l)} R_c}{\partial r^{\alpha(l)}} \cdot \frac{\partial^{\gamma(l)} R_e}{\partial r^{\gamma(l)}} dr \right\} \left\{ \int_0^{2\pi} \frac{\partial^{\beta(l)} \Phi_d}{\partial \varphi^{\beta(l)}} \cdot \frac{\partial^{\delta(l)} \Phi_f}{\partial \varphi^{\delta(l)}} d\varphi \right\} = D \sum_{l=1}^{15} I_{kr}(l) \cdot I_{kphi}(l) \quad (6)$$

Indexes of the matrix  $\mathbf{M}$  are  $c(i) = 1 + (i-1)\%m$ ,  $e(j) = 1 + (j-1)\%m$ ,  $d(i) = 1 + [(i-1) - (i-1)\%m]/m$ ,  $f(j) = 1 + [(j-1) - (j-1)\%m]/m$ , where  $\%$  is the modulo operator (the remainder of division of one integer number by another). Matrix  $\mathbf{K}$  is a sum of 17 components due to the complexity of  $V$  function, where  $\alpha, \beta, \gamma, \delta, f$  can take the value 0, 1 or 2 and  $c$  can be substituted by 1,  $2 \cdot (1-\nu)$ ,  $-2 \cdot (1-\nu)$  or  $-(1-\nu)$ . Variables  $\alpha, \beta, \gamma, \delta, f, c$  depends on  $l$  according to Table 1.

$l$	1	2	3	4	5	6	7	8	9	10	11	12	13	14	15	16	17
$c$	1	1	1	1	1	1	1	1	1	2 \cdot (1-\nu)	-2 \cdot (1-\nu)	-2 \cdot (1-\nu)	2 \cdot (1-\nu)	-(1-\nu)	-(1-\nu)	-(1-\nu)	-(1-\nu)
$\alpha$	2	2	2	0	0	0	1	1	1	1	1	0	0	2	2	0	1
$\beta$	0	0	0	2	2	2	0	0	0	1	1	1	1	0	0	2	0
$\gamma$	2	0	1	2	0	1	2	0	1	1	0	1	0	0	1	2	2
$\delta$	0	2	0	0	2	0	0	2	0	1	1	1	1	2	0	0	0
$f$	0	2	1	2	4	3	1	3	2	2	3	3	4	2	1	2	1

Table 1: Values of  $c, \alpha, \beta, \gamma, \delta$  and  $f$  for each index  $l$

Considering Eq. (4) of the undamped system, we can calculate the natural frequencies  $f$  of the system by computing the eigenvalues  $\lambda$  of  $\mathbf{M}^{-1} \mathbf{K}$  [14].

$$f = \frac{\omega}{2\pi} = \frac{\sqrt{\lambda}}{2\pi} \quad (7)$$

### 3 NUMERICAL INTEGRATION OF B-SPLINES

B-splines are mostly used for interpolating and gives good results even when using low degree polynomials. A B-spline function is a defined piecewise polynomial of degree  $k$ , which is static at the crossing segment  $C^{k-1}$ . For cubic B-splines, it means  $k=3$ , the continuity of the curvature is warranted. Hence it can approximate the geometrical form of an elastic deformed body, for example the bending of a bar or a bending plate.

To define a set of B-splines  $R_{i,k+1}(r)$  we need a vector of knots  $\vec{t} = \{t_1, t_2, \dots, t_n\}$  and the degree  $k$  [15].

$$k=0, R_{i,0}(r) = \begin{cases} 1, & t_i \leq r < t_{i+1} \\ 0, & \text{else} \end{cases} \quad (8)$$

$$k > 0, R_{i,k}(r) = \frac{r-t_i}{t_{i+k}-t_i} R_{i,k}(r) + \frac{t_{i+k+1}-r}{t_{i+k+1}-t_{i+1}} R_{i+1,k}(r)$$

If the number of B-splines is  $m$ , the size of the vector  $\vec{t}$  is  $n = m + k + 1$ . In order to attend the recursive formula that evaluate the B-splines, the  $k+1$ -first elements of  $\vec{t}$  are equal to the first element  $t_1$ , i.e.  $t_1 = \dots = t_{k+1}$  and the last  $k+1$  elements of  $\vec{t}$  are equal to the last element  $t_n$ , i.e.  $t_{n-k} = \dots = t_n$ . In this approach, knots divide the length between  $r=b$  and  $r=a$  in equal segments and  $t_1 = b$  and  $t_n = a$ . Fig. 2 shows seven cubic B-splines generated for  $\vec{t}_4 = \{0, 0, 0, 0, \frac{1}{4}, \frac{2}{4}, \frac{3}{4}, 1, 1, 1, 1\}$ . For cubic B-splines ( $k=3$ ):

$$R_{i,3}(r) = \begin{cases} \frac{(r-t_i)^3}{(t_{i+3}-t_i)(t_{i+2}-t_i)(t_{i+1}-t_i)}, & t_i \leq r < t_{i+1} \\ \frac{(r-t_i)(t_{i+3}-r)(r-t_{i+1})}{(t_{i+2}-r)(r-t_i)^2} + \frac{(r-t_i)(t_{i+3}-r)(r-t_{i+1})}{(t_{i+3}-t_{i+1})(t_{i+3}-t_i)(t_{i+2}-t_{i+1})} \\ + \frac{(t_{i+4}-r)(r-t_{i+1})^2}{(t_{i+4}-t_{i+1})(t_{i+3}-t_{i+1})(t_{i+2}-t_{i+1})}, & t_{i+1} \leq r < t_{i+2} \\ \frac{(r-t_i)(t_{i+3}-r)^2}{(t_{i+3}-t_i)(t_{i+2}-t_{i+1})(t_{i+3}-t_{i+2})} + \frac{(r-t_{i+1})(t_{i+3}-r)(t_{i+4}-r)}{(t_{i+4}-t_{i+1})(t_{i+3}-t_{i+1})(t_{i+3}-t_{i+2})} \\ \frac{(r-t_{i+2})(t_{i+4}-r)^2}{(t_{i+4}-t_{i+1})(t_{i+4}-t_{i+2})(t_{i+3}-t_{i+2})}, & t_{i+2} \leq r < t_{i+3} \\ \frac{(t_{i+4}-r)^3}{(t_{i+4}-t_{i+1})(t_{i+4}-t_{i+2})(t_{i+4}-t_{i+3})}, & t_{i+3} \leq r < t_{i+4} \\ 0, & \text{else} \end{cases} \quad (9)$$

From Eq. (5),  $I_{mr}$  is a integration of cubic B-splines, i. e.,  $R_i(r)$  is a polynomial function with degree of 3. That way,  $I_{mr}$  is the integration of a 7-degree piecewise polynomial.

$$I_{mr} = \int_b^a R_c(r) \cdot R_e(r) \cdot r \cdot dr = \sum_{i=1}^{n-1} \int_{r=t_i}^{t_{i+1}} R_c(r) \cdot R_e(r) \cdot r \cdot dr \quad (10)$$

Gaussian quadrature rule is used to convert an integral into a sum of function values at specified points within the domain of integration. Eq. (11) shows Gaussian quadrature rule applied to  $I_{mr}$ . The same approach can be used in order to calculate  $I_{kr}(l)$ .

$$I_{mr} = \sum_{i=1}^{n-1} \sum_{p=1}^7 H_p \cdot R_c(\hat{g}_p) \cdot R_e(\hat{g}_p) \cdot \hat{g}_p \cdot \left( \frac{t_{i+1} - t_i}{2} \right) , \quad \hat{g}_p = \left( \frac{t_{i+1} - t_i}{2} \right) \cdot g_p + \left( \frac{t_{i+1} + t_i}{2} \right) \quad (11)$$

$\pm g$	$H$
0.949107912342759	0.129484966168870
0.741531185599394	0.279705391489277
0.405845151377397	0.381830050505119
0.000000000000000	0.417959183673469

Table 2: Gaussian quadrature constants for 7-degree polynomial.

#### 4 CLOSED-FORM SOLUTION OF THE PLATE DYNAMICS

Annular plates have high degree of symmetry and their modes of vibration have closed-form solutions, expressed in trigonometric functions in angular coordinate ( $\varphi$ ) and Bessel functions in radial coordinate ( $r$ ) [1].

$$z(r, \varphi, t) = \left[ a_{ij} J_i \left( \frac{\xi_{ij} r}{a} \right) + b_{ij} Y_i \left( \frac{\xi_{ij} r}{a} \right) + c_{ij} I_i \left( \frac{\xi_{ij} r}{a} \right) + d_{ij} K_i \left( \frac{\xi_{ij} r}{a} \right) \right] \cos(i\varphi) \sin(2\pi ft) \quad (12)$$

Where  $i, j = 0, 1, 2, 3, \dots$   $J_i$  and  $Y_i$  are Bessel functions of the first and second kinds and  $i$  order.  $I_i$  and  $K_i$  are modified Bessel functions of the first and second kinds and  $i$  order and  $a_{ij}$ ,  $b_{ij}$ ,  $c_{ij}$ , and  $d_{ij}$  are constants determined by the boundary conditions and mode numbers  $i$  and  $j$ .

The dimensionless frequency parameter  $\xi$  is a function of the boundary conditions on the plate, the ration of the inner to outer diameter of the plate and the Poisson ratio  $\nu$ . The parameter  $\xi$  is determined by setting the determinant of the characteristic matrix to zero to impose the desired boundary conditions on the general solution. The result of this transcendental equation is an infinite number of solutions  $\xi$ , which are associated with the mode numbers  $i$  and  $j$ . The natural frequencies  $f$  are calculated as function of the dimensionless parameter  $\xi$ . The parameter  $\xi^2$  is showed in Table 3, considering  $\nu = 0.3$  and  $b/a = 0.5$ .

Free-Free		Supported-Free		Clamped-Free	
B-spl.	CFS	B-spl.	CFS	B-spl.	CFS
4.271	4.28	4.121	4.11	13.02	13.0
4.271	4.28	4.862	4.86	13.29	13.3
9.314	9.32	4.862	4.86	13.29	13.3
11.43	11.4	7.986	7.98	14.70	14.7
11.43	11.4	7.986	7.98	14.70	14.7
17.20	17.2	14.04	14.0	18.56	18.5
17.20	17.2	14.04	14.0	18.56	18.5

Table 3: Dimensionless eigenfrequencies  $\xi^2$  using B-splines discretization and Closed-form solution (CFS)

$$f = \frac{\xi^2}{2\pi a^2} \left( \frac{D}{\rho h} \right)^{1/2} = \frac{\xi^2 h}{2\pi a^2} \left( \frac{E}{12\rho(1-\nu^2)} \right)^{1/2} \quad (13)$$

## 5 VALIDATION OF ANNULAR PLATE NATURAL FREQUENCIES

In order to compare and validate the results of the analytical model using B-spline functions and the closed-form solution, it was used the Finite Element Method (FEM) and a modal testing of a real annular plate.

The Finite Element Method (FEM) [16] is an approximation method for studying continuous physical systems largely used in structural mechanics. The system is broken into discrete elements interconnected at discrete node points. In the discretization of the annular plate, each shell element has eight nodes with six degrees of freedom at each node: translations in the x, y, and z axes, and rotations about the x, y, and z axes. Mindley-Reissner plate theory [10-11] is used in order to model the equations governing the element deformation and motion.

Modal Testing is a form experimental testing that measures the vibration of a structure compared to a knowed excitation. Impact hammer testing and shaker (vibration tester) testing are the most common kinds of excitation.

Natural frequencies of the plate are very sensible to the exciter and measurer because it has a mass of only 206.5 g. Measurement using accelerometers could add considerable mass to the system and change the results. The same way, a shaker exciter could have a considerable mass added by its force sensor between the shaker and the plate. In order to avoid these problems, it was used a laser velocimeter to measure the displacement of the plate and a hammer blow to excite the plate vibration.

Impact hammer provides a force similar to a Dirac delta in the time domain, causing a constant amplitude in the frequency domain. Natural frequencies are found by identifying the peaks of the Frequency Response Function (FRF) of the measured velocity of the plate point and the excitation force [14]. In order to simulate Free-Free boundary conditions, the plate is suspended by thin elastic wires.



Figure 3: Modal testing using hammer blow for excitation and laser velocimeter for measurement (red point).

The geometric parameters of the annular plate are  $h=0.00315m$  ,  $b=0.050m$  , and  $a=0.100m$  and it is made of aluminium with  $\rho=2780kg/m^3$  ,  $E=7.24 \cdot 10^{10} N/m^2$  , and  $\nu=0.33$  .

B-splines	FEM	Modal Testing	Bspl- MTest	FEM-MTest	Bspl - FEM
329.7	328.1	327.2	0,8%	0,3%	0,5%
329.7	328.1	327.2	0,8%	0,3%	0,5%
722.8	721.3	731.4	-1,2%	-1,4%	0,2%
882.4	877.7	880	0,3%	-0,3%	0,5%
882.4	877.7	880	0,3%	-0,3%	0,5%
1327	1303	1310	1,4%	-0,5%	1,9%
1327	1303	1310	1,4%	-0,5%	1,9%
1628	1616	1619	0,5%	-0,2%	0,7%
1628	1616	1619	0,5%	-0,2%	0,7%

Table 4: Comparison of Annular plate natural frequencies (Hz).

## 6 CONCLUSIONS

- Analytical modeling using B-splines for discretization showed in this work successfully found the same eigenfrequencies as the Closed-Form Solution of a annular plate without spending computational time for calculating Bessel functions.
- Analytical modeling using B-splines for discretization provides a general algorithm for choosing Boundary conditions (Free, Supported, and Clamped) by excluding some B-spline functions. It is much more general than the Closed-Form Solution that have an different characteristic equation for each of the 9 possible boundary conditions.
- The advantage of this analytical method using B-splines is to present an alternative solution apart from importing mass and stiffness matrix generated by a FEM software or solving complicated transcendental equation evolving Bessel functions from the CFS.
- The bigger is the number of functions used in the discretization, the bigger the number of natural frequencies found, and the more accurate will be the approximation. The method developed presents a good convergence of the solution.
- The natural frequencies calculated B-splines for discretization successfully fit those frequencies calculated using the Closed-Form Solution and are 0.5% to 2% bigger than those calculate using FEM. The small difference between the results occurs because FEM uses Mindley-Reissner plate theory and the analytical methods use classical Kirchoff plate theory. Mindley-Reissner theory considers shear strain and classical plate theory consider strain deformation is null.
- According to Eq. (13), natural frequencies increases with the thickness and decrease with the square of the radius, i.e., if we maintain the same proportion, the bigger is the disc, the smaller are the natural frequencies. Aluminium discs and steel discs have almost the same natural frequencies, because the change in Young's Modulus  $E$  is compensated by the change in the density.
- FEM and Analytical modeling using B-Splines successfully fit measured frequencies in the Modal Testing with a difference of 0.5% to 2%. Impact hammer is a best modal testing excitation than shaker for light structures.



## 7 ACKNOWLEDGEMENTS

The authors thank CAPES (Coordenação de Aperfeiçoamento de Pessoal de Nível Superior) for promoting and supporting this research.

## REFERENCES

- [1] R.D. Bleviss, *Formulas for natural frequency and mode shape*. Krieger Pub Co, 1995.
- [2] S.S. Rao, A. S. Prasad, Vibration of annular plates including the effects of rotary inertia and transverse shear deformation, *Journal of Sound and Vibration* 42 , 305-324, 1975.
- [3] S.M. Han, H. Benaroya and T. Wei, *Dynamics of Transversely Vibrating Beams using four Engineering Theories*. Academic Press. Retrieved 2007-04-15, 1999.
- [4] G. Kirchhoff, Über das Gleichgewicht und die Bewegung einer elastischen Scheibe, *Journal für die reine und angewandte Mathematik*, Vol. 40, No. 1, pp.51-88, 1850.
- [5] A.E.H. Love, On the small free vibrations and deformations of elastic shells, *Philosophical trans. of the Royal Society* (London), Vol. série A, N° 17 p. 491–549, 1888.
- [6] A. E. H. Love, *A treatise on the mathematical theory of elasticit*, 4th ed, 1926.
- [7] H. Lamb, *The dynamical theory of sound*, 2nd ed, 1925.
- [8] J.W.S. Rayleigh, *The theory of sound*, London: Macmillan and co, 1877.
- [9] S.P. Timoshenko, *Vibration problems in engineering*, 1st ed., New York: D Van Nostrand Co, 1928.
- [10] R.D. Mindlin, Influence of rotatory inertia and shear on flexural motions of isotropic, elastic plates, *ASME Journal of Applied Mechanics*, Vol. 18 pp. 31–38, 1951.
- [11] E. Reissner. *The effect of transverse shear deformation on the bending of elastic plates*, *J. Appl. Mech.*, 12, 69–77, 1945.
- [12] A.W. Leissa, *Vibration of Plates*, NASA SP-160, Office of Technology Utilization, Washington D.C., 353p, 1969.
- [13] R. Szilard, *Theory and Analysis of Plates: Classical and Numerical Methods*. Prentice-Hall. 724 p, 1973.
- [14] D. J. Ewins, *Modal Testing: Theory, Practice and Application*, 2<sup>nd</sup> ed., Research Studies Press Ltd., Baldock, England, 2000.
- [15] A. Heckmann, *Programmbibliothek zur simulation elastischer Mehrkörpersysteme*. Munich, Germany: Diplomarbeit – Technische Universität München, 1999.
- [16] O.C. Zienkiewicz, and R.L. Taylor, *The Finite Element Method. Volume 1: The Basis*. 5th ed. Oxford, UK: Butterworth-Heinemann. 689 p, 2000.